Optical and electronic properties of Ag nanodots on Si(111)

2006 J. Phys.: Condens. Matter 18 6979

(http://iopscience.iop.org/0953-8984/18/30/003)

INSTITUTE OF PHYSICS PUBLISHING JOURNAL OF PHYSICS: CONDENSED MATTER

J. Phys.: Condens. Matter **18** (2006) 6979–6986 doi:10.1088/0953-8984/18/30/003

Optical and electronic properties of Ag nanodots on Si(111)

S Chandola[1], J Jacob[1], K Fleischer[1,2], P Vogt[2], W Richter[2] and J F McGilp[1,3]

[1] School of Physics, Trinity College Dublin, Dublin 2, Republic of Ireland
[2] Technische Universität Berlin, Institut für Festkörperphysik, Sekretariat, PN 6-1, Hardenbergstraße 36, D-10623 Berlin, Germany

E-mail: jmcgilp@tcd.ie

Received 20 April 2006, in final form 1 June 2006
Published 14 July 2006
Online at stacks.iop.org/JPhysCM/18/6979

Abstract

Reflectance anisotropy spectroscopy (RAS) has been used, together with scanning tunnelling spectroscopy (STS), to investigate the optical and electronic properties of nanodots formed by depositing Ag on the Si(111)–3 × 1-Ag surface. One-dimensional (1D) arrays of nanodots were grown on a single-domain (3 × 1)-Ag surface and the anisotropic optical response in the 0.5–5 eV range measured by RAS. Aligned, elongated Ag islands were also grown on this surface to compare their properties with those of the nanodots. STS of the Ag islands showed distinct metallic behaviour, whereas the nanodots revealed a bandgap of ∼0.6 eV, indicating that the surface of the dots has a non-metallic character, similar to that of the Si(111)–3 × 1-Ag surface. RAS also showed substantial differences between the structures, with a large infrared anisotropy for the metallic Ag islands consistent with anisotropic Drude-like intraband transitions, whereas the nanodots gave a negligible response in this spectral region. The RAS results in the infrared spectral region are consistent with the difference in the metallic character of the nanodots and islands, as determined by STS.

1. Introduction

Low-dimensional structures arising from metal adsorption on semiconductor surfaces can exhibit unusual physical phenomena and have attracted considerable interest in recent years. Si(111) and its vicinal surfaces, in particular, have shown a variety of chain structures after depositing sub-monolayer quantities of metal atoms. In [1] and Au ([2, 3] and references therein) form *quasi*-one-dimensional (1D) metallic chains, but semiconducting structures can

[3] Author to whom any correspondence should be addressed.

also be formed. One of the best known of these metal-induced reconstructions is the Si(111)–3 × 1-X structure, which is formed by various adsorbates, X, such as the alkali metals (Li, Na, K), the alkaline-earth metals (Mg, Ca, Ba), the rare-earth metals (Sm, Yb), and Ag, at a coverage of a 1/3 monolayer (ML).

The Ag/Si interface has been studied in great detail for both fundamental and technical reasons, one of them being that Ag does not diffuse into the Si bulk, resulting in an abrupt interface. The reconstructions at the surface are still a subject of considerable interest. Whereas the $(\sqrt{3} \times \sqrt{3})$-Ag reconstruction is now well established, significant questions remain about the (3 × 1)-Ag surface. Several models have been proposed for the metal-induced (3 × 1) reconstruction, with the most favoured one currently being the honeycomb chain-channel (HCC) model [4–6], which exhibits the lowest energy of any of the proposed structures to date [6]. The model also predicts a double bond between the two closest Si atoms on the surface, which is unusual. The electronic structure of the (3 × 1)-Ag surface has been studied by angle resolved photoemission (ARPES) for the three-domain [7] and the single-domain [8] surfaces. Both these studies concluded that the (3 × 1)-Ag surface has a semiconducting character, as no photoemission intensity was detected at the Fermi level in either crystallographic direction. The ARPES measurements on the single-domain surface found that there are at least two surface states parallel to the chains and also at least two in the orthogonal direction.

It has been reported [9, 10] that 1D arrays of Ag quantum dots, aligned along the ⟨110⟩ chain direction, can be grown at room temperature (RT) using the (3 × 1)-Ag surface as a template. The nanodots nucleate in the trenches between the Ag chains of the HCC structure and appear to be monodisperse. The dots are 1 nm in diameter by 0.15 nm in height and contain an estimated 19 atoms [9]. Above ∼0.5 ML Ag, the self-assembling nucleation of the nanodots breaks down and larger three-dimensional (3D) islands start growing [9].

In this work, the optical and electronic response of the Si(111)–3 × 1-Ag surface, and of nanodots and larger islands grown on this surface, have been studied with reflectance anisotropy spectroscopy (RAS), and scanning tunnelling microscopy (STM) and spectroscopy (STS). The RAS results in the infrared spectral region are consistent with the difference in the metallic character of the nanodots and islands determined by STS and, together, these two techniques, with their different sampling depths, provide good evidence that the nanodots are non-metallic.

2. Experiment

The experiment was carried out in an ultrahigh-vacuum (UHV) chamber, with a base pressure of $\sim 1 \times 10^{-10}$ mbar, equipped with an Omicron STM and low-energy electron diffraction (LEED) system. The vicinal Si(111) sample was n-type, phosphorous doped, with a resistivity in the range 0.1–20 Ω cm, offcut by 1° towards the $[\bar{1}\bar{1}2]$ direction. Using the procedure detailed by O'Mahony *et al* [11], direct current heating of the sample produced a regular array of single height steps, with a sharp 7 × 7 LEED pattern forming after cooling. The clean Si(111) surface was exposed to less than 1 ML of Ag, at a substrate temperature of 870 K. RAS was used to follow the growth of Ag on the surface and, by monitoring an RAS transient at 2.2 eV, a mostly single-domain Si(111)–3 × 1-Ag surface could be grown quite easily. The RAS feature at this energy is directly related to the formation of the 3 × 1 surface, with the intensity depending on the excess of the single-domain structure over the other two symmetry-related domains. A single-domain 3 × 1 LEED pattern was observed over most of the surface, with the atomic chains aligned in the direction of the step edges, together with some $(\sqrt{3} \times \sqrt{3})$ features appearing at the edges of the sample. Using the 3 × 1 surface as a template, an additional approximately 0.5 ML of Ag was deposited at RT to form 1D arrays of nanodots, aligned along the ⟨110⟩ chain direction. The nanodots were very uniform in size, 1 nm in diameter by 0.2 nm

in height, and nucleated in the trenches between the Ag chains, in agreement with previous work [9, 10]. LEED showed that the single-domain 3 × 1 pattern was still preserved, but the spots were slightly diffuse. Lastly, larger Ag islands were formed by further deposition of up to 2 ML of Ag at RT. The whole procedure, from clean Si(111) to larger Ag island formation, together with the various experimental measurements, was repeated a number of times to ensure reproducibility of results.

RAS measures the difference in reflectance, at near normal incidence, of light linearly polarized in two orthogonal directions at the surface plane of a cubic material [12, 13]. The real part of the anisotropy in the reflection coefficients normalized to the average reflection coefficient, Re$[\Delta r/r]$, is related to the surface and bulk dielectric function components by:

$$\mathrm{Re}\left[\frac{\Delta r}{r}\right] = \frac{4\pi d}{\lambda}\mathrm{Im}\left[\frac{\varepsilon_{1\bar{1}0} - \varepsilon_{\bar{1}\bar{1}2}}{\varepsilon_{\mathrm{b}} - 1}\right] \tag{1}$$

where d is the overlayer thickness, λ is the wavelength of the light, $\varepsilon_{1\bar{1}0}$ and $\varepsilon_{\bar{1}\bar{1}2}$ are the surface dielectric function components parallel and perpendicular to the steps, respectively, and ε_{b} is the bulk dielectric function. The RAS apparatus is unusual in having the energy range extended to 0.5 eV (most RAS systems are limited to 1.5 eV by the photomultiplier detectors used). The extended energy range, from infrared (IR) to visible (vis) and near ultraviolet, is expected to be particularly useful for probing low-dimensional metallicity [14]. The IR–vis RAS instrument utilizes MgF_2 polarizers, a CaF_2 photoelastic modulator, and a double-grating monochromator, one for the IR and one for the near-infrared (NIR) to UV range, with three detectors: a liquid nitrogen cooled InAs detector for measurements between 0.45 and 0.9 eV, an InGaAs photodiode for 0.75–1.5 eV, and a Si photodiode for measurements above 1.3 eV. The effective range is 0.5–5 eV with these components and the fused silica window of the UHV system.

After the RAS measurements, the sample was transferred to the STM part of the UHV chamber, where STM and STS was carried out at room temperature. STS provides the desired sensitivity and spatial resolution, making it possible to carry out tunnelling spectroscopy measurements on individual nanodots. All imaging and spectroscopy were performed using electrochemically etched tungsten tips. In order to correlate I–V spectra with topographical features on the surface, the spectra were taken in a grid pattern at every fifth point (0.5 nm spacing) during the simultaneous acquisition of an STM topograph.

3. Results and discussion

Figure 1 shows RAS spectra during the growth of Ag on the clean, vicinal Si(111)–7×7 surface. Defects and disorder in the surface, and any domain averaging, will reduce the anisotropy of the signal. The very small spectral features near 3.4 and 4.2 eV for the clean surface arise from step-modified bulk optical transitions across the direct silicon band gap, similar to those published by Yasuda *et al* [15]. The RAS spectrum for the Si(111)–3 × 1-Ag surface is dominated by the negative feature at 2.2 eV, indicating a dominant polarizability in the $[\bar{1}\bar{1}2]$ direction, orthogonal to the chain and step direction. The 2.2 eV feature is unambiguously related to surface and interface states, as this energy region is far below the direct optical gap of Si. A differential photoreflectance spectroscopy study of singular Si(111)–7 × 7-Ag, Si(111)–$\sqrt{3} \times \sqrt{3}$-Ag, and Si(001)-2 × 1-Ag interfaces has also reported a wide peak around 2.3 eV, with the dominant polarizability in the $[\bar{1}\bar{1}2]$ direction [16]. The 2.2 eV feature showed a small decrease in intensity after one week in UHV, with LEED still showing a single-domain 3 × 1 structure, although the 3× spots were not as sharp. This indicates that there are a number of transitions contributing to this feature, with only some of them being affected by light surface

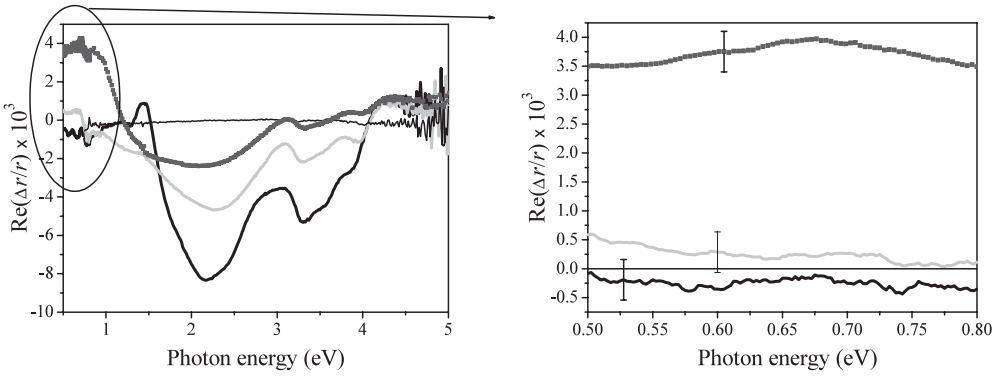

Figure 1. Left: RAS of the formation of Si(111)–3 × 1-Ag and subsequent growth of Ag on the (3 × 1) surface: Si(111)–7 × 7 (thin black line); Si(111)–3 × 1-Ag (thick black line); 0.5 ML Ag on Si(111)–3 × 1-Ag (thick grey line); 2 ML Ag on Si(111)–3 × 1-Ag (black dots). Right: expanded image of the 0.5–0.8 eV region. The experimental uncertainty of the zero line is indicated by the error bar.

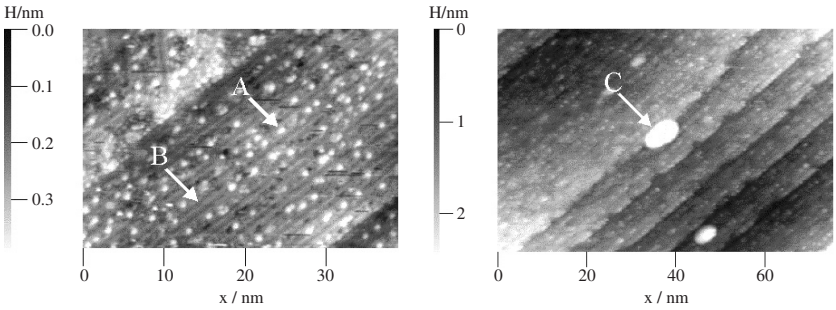

Figure 2. Left: STM image of nanodots, 0.2 nm in height, grown on the Si(111)–3 × 1-Ag surface. An example of a nanodot is shown at A. An area of reconstructed (3 × 1) surface is shown at B. Right: STM image of an elongated 3D Ag island (C), 1.5 nm in height, with its long axis aligned along the steps. The sample bias voltage was 1.1 V and the tunnelling current was 0.2 nA.

contamination. The 2.2 eV feature has been discussed in detail in a previous paper, in relation to other chain-like structures that form on the vicinal Si(111) surface [17].

Identifiable and reproducible structures also appear at 1.4, 2.5, 3.3, 3.6 and 3.9 eV. Between 0.5 and 0.9 eV, the RAS response from the 3 × 1 surface is very small and negative. All measurements in this energy range were averaged over 10 spectra for each different surface reconstruction in order to reduce the estimated error of $\sim 5 \times 10^{-4}$ arising from noise and zero-level uncertainty, but the small negative value is still comparable to the estimated offset error associated with residual misalignment of the two polarizers.

Deposition of an additional 0.5 ML of Ag at RT then led to the formation of nanodots on the 3 × 1 surface (figure 2 left). Although the RAS structures between 1.4 and 3.9 eV showed significant attenuation and some modification (figure 1 left), the infrared RAS response only showed a very small positive anisotropy, increasing slightly towards lower energies (figure 1 right). More Ag was then deposited at RT, up to approximately 2 ML, in order to determine the RAS response in the coverage régime where larger Ag islands are formed. Further attenuation of the RAS structures between 1.4 and 3.9 eV was observed (figure 1), but now a large positive response can be seen in the IR, which appears to plateau below 0.8 eV. STM measurements

show that isolated, elongated Ag islands, of height ∼1.5 nm, have been formed, with their long axis aligned in the direction of the step edges (figure 2 right, C). The RAS instrument can also measure the polarization-averaged IR reflectivity, but no significant, reproducible changes were observed between the different structures.

Electronic structure calculations are beginning to be extended to include the determination of the anisotropic linear optical response, as has been accomplished recently for the Si(111)–4 × 1-In system [18]. A detailed interpretation of the spectral features in figure 1 must await realistic calculations of the Si(111)–3 × 1-Ag surface, but progress can be made in interpreting the infrared response. Metallic conductors have a Drude-like intraband contribution to the optical conductivity in the infrared spectral region [19]. For bulk Ag, where there are no significant bulk interband optical transitions below ∼3 eV, the Drude contribution becomes significant below about 1 eV ([20], and references therein). The large positive IR response at higher coverages, with the dominant polarizability along $[1\bar{1}0]$, the direction of the long axis of the islands, is in the spectral region where anisotropic Drude-like intraband transitions begin to make a significant contribution to the optical spectrum. The simplest explanation for the optical response being sensitive to the shape of the islands is that the inelastic scattering mean free path (mfp) of conduction electrons in bulk Ag at RT is ∼60 nm [21], resulting in the mfp of the optically excited conduction electrons being determined by the island dimensions. A simple anisotropic Drude model [22] with scattering lengths determined by the dimension of these nanoscale islands is sufficient to produce the positive anisotropy in the response that is observed. The plateau indicates that anisotropic surface interband transitions may still be contributing to the response, and percolation effects may also have to be considered [23]. It is clear that the spectral region will need to be extended further into the IR to explore the nature of the plateau.

For the lower coverages, the (3 × 1)-Ag surface, with and without nanodots, shows a very small response below 1 eV (figure 1). The 3 × 1 surface is known to be semiconducting [7, 8], and the optical response is consistent with the absence of metallic character. The lack of such a response from the nanodots, which are monodisperse and are estimated to contain 19 Ag atoms [9], is interesting. While it is possible that the nanodots, although aligned in chains (figure 2 left) and separated by only ∼1.5 nm, produce a negligible anisotropic response because their shape is isotropic, it is more likely that the Ag nanodots are, in fact, non-metallic.

In order to resolve this question, STS measurements were conducted on Si(111)–3 × 1-Ag, nanodot and 3D island surfaces. All STS spectra were averaged over several individual spectra taken along relevant structures to improve the signal-to-noise ratio. The tip was also scanned between the dots parallel and perpendicular to the linear arrays to see if there was any difference in the tunnelling spectra. Tunnelling spectra from the (3 × 1)-Ag surface, the nanodots, and the Ag islands, are shown in figure 3 left. STS on the (3 × 1) surface showed a bandgap of ∼1.1 eV, clearly indicating the semiconducting state of this surface. In contrast, the Ag islands showed unambiguous metallic behaviour, with a straight line through the zero point (figure 3 left C, with change of scale), consistent with the observation of the Drude tail in the optical spectra of figure 1. STS on the nanodot surface, however, reveals a small bandgap of ∼0.6 eV, indicating non-metallic character, again consistent with the absence of a Drude tail in the optical spectra. STS measurements between two nanodots in the same line, and between two nanodots in adjacent lines, showed a small anisotropy, with the inter-dot bandgap of the former being smaller by about 0.2 eV (figure 3 right).

The electronic properties of metallic nanoclusters grown on substrates depend on the metal, the size and shape of the cluster, and the substrate. When the size of a cluster is less than a few nanometres, the electronic states become discrete, due to confinement of the electron wavefunction. The average spacing of successive quantum levels, δ, known as the Kubo gap, is

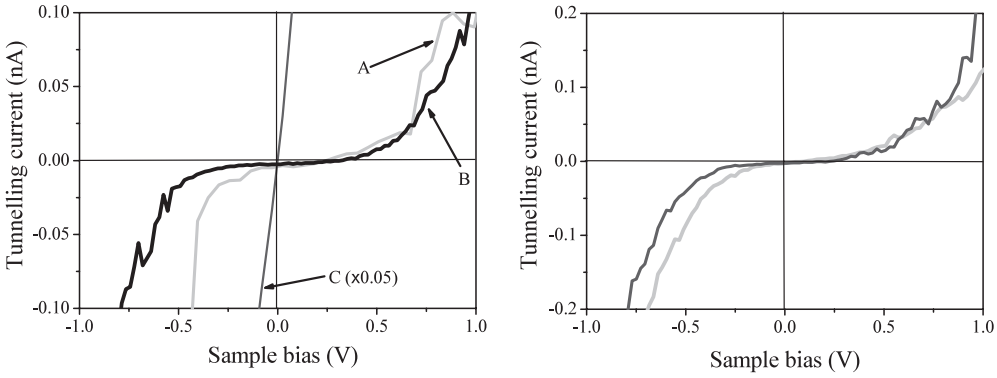

Figure 3. Left: STS spectra of the nanodots (A), the (3 × 1)-Ag surface (B), and the 3D Ag islands (C, with change of scale). Right: STS spectra taken between two nanodots in the same line (thick grey line) and between two nanodots in adjacent lines (thick black line).

given by $\delta = 4E_f/3n$, where E_f is the Fermi energy of the bulk metal and n is the number of valence electrons in the cluster [24]. Thus, for the Ag nanodots containing about 19 atoms [9], the value of δ would be ∼0.4 eV. This size-induced metal–insulator transition in nanoclusters has been observed, using STS, for several metals, such as Au, Pd, Ni and Ag, on a variety of substrates [24, 25]. Clusters of less than 2 nm diameter tend to be two-dimensional (2D) and non-metallic, and there is evidence that metallicity develops in larger nanoclusters as the particles become 3D in character [25]. Isolated 2D Ag nanodots of the size observed are thus expected to be non-metallic. In contrast, the larger islands that form after the nanodot phase ('C' in figure 2) contain ∼1000 atoms, resulting in a negligible Kubo gap and metallic behaviour.

Where the nanoclusters are not isolated, however, there is evidence that lateral interactions between clusters can induce metallic behaviour. In an STS study of Ag nanoclusters on Si(100), it was found that the lateral conduction between neighbouring Ag clusters contributed significantly to the I–V characteristics via coupling through the substrate [26]. A study of coupling interactions as a function of inter-particle separation, using a monolayer of organically functionalized Ag nanoclusters, found that a metal–insulator transition occurred when $D/2r < 1.2$, where D is the distance between the centres of adjacent dots and $2r$ is the diameter of the dot [21]. The nanodots (figure 2 left) self-assemble such that, on average, $D/2r \sim 2.2$–3.2 [9] and thus the nanodots are not sufficiently close for lateral conduction to render them metallic.

There is another, albeit remote, possibility that should be considered. STM does not reveal atomic character directly, and STS is extremely surface sensitive. It is possible that the nanodots are Si adatoms, displaced by Ag atoms that embed in the surface beneath the dots, and that the embedded Ag cluster is metallic but not probed by STS. The displacement of Si atoms by Au to produce Si adatoms has been observed previously on Si(111) surfaces [26], but the displacement mainly produces isolated adatoms. Other low-dimensional systems grown on Si have not shown this behaviour [27], making the displacement of Si in 19 atom patches highly unlikely. It is important to note that the larger sampling depth of the RAS technique would detect the Drude signature of such embedded, aligned metallic Ag clusters, assuming the optical response was anisotropic. Care is required in interpretation, however, as an optically isotropic Drude tail of a buried metallic cluster would not be detected by RAS.

Finally, it has been suggested that the remarkably uniform 2D clusters form because a hexagonal Ag(111) packing arrangement with 19 Ag atoms just fits between neighbouring Ag channels of the HCC structure of the Si(111)–3 × 1-Ag surface [9]. It is not clear, however, why

the nanodots do not elongate along the channels by adding further Ag atoms. For unsupported clusters of around this size, the formation of super-atom spherical clusters of 8, 20 and 40 atoms is favoured for monovalent atoms, because of the additional stability associated with closed quantum shells arising from surface quantization, and such super-atom clusters have been observed experimentally [28]. Interaction with the underlying (3×1)-Ag surface clearly modifies this behaviour, because only 2D nanodots form at this coverage. It thus appears unlikely that super-atom considerations influence the cluster size, although this may be possible if the surface interactions are particularly finely balanced in this system.

4. Conclusion

Two-dimensional Ag nanodots of 1 nm diameter have been grown by self-assembly on the Si(111)–3×1-Ag surface, in rows running parallel to the steps of the vicinal surface. STS has shown that the clusters are non-metallic, with a bandgap of $\sim$0.6 eV, consistent with the opening of a Kubo gap due to confinement of the electron wavefunction. This is expected for such small clusters, provided that their separation is at least comparable to their dimension, thus reducing lateral interactions. Larger, anisotropic 3D Ag islands, formed by further deposition of Ag, also align along the rows, but STS has shown these to have well-developed, metallic character, in agreement with their larger size. RAS measurements extended into the IR region have been shown to be consistent with the electronic properties of the nanostructures measured by STS. The large positive IR anisotropy for the 3D Ag islands is in the region where anisotropic Drude-like intraband transitions begin to become significant, the larger polarizability being aligned along the length of the islands, where the inelastic scattering electron mean free path is expected to be longer. In contrast, the nanodots show a very small optical response in the IR region, which is consistent with their non-metallic character. The agreement between the electronic properties, as measured by STS, and the IR measurements indicates that infrared RAS should be a useful technique for the non-contact probing of the metallicity of aligned anisotropic nanostructures. The penetration depth of this optical technique is such that technologically useful buried nanostructures protected by thin capping layers should also be accessible.

Acknowledgments

Financial support for this work was provided by the Irish Higher Education Authority and IRCSET Grant No SC/2003/223/. Theo Herrmann and Matthias Wahl are thanked for the initial construction of the infrared RAS system.

References

[1] Yeom H W, Takeda S, Rotenberg E, Matsuda I, Horikoshi K, Schaefer J, Lee C M, Kevan S D, Ohta T, Nagao T and Hasegawa S 1999 *Phys. Rev. Lett.* **82** 4898
[2] Collins I R, Moran J T, Andrews P T, Cosso R, O'Mahony J D, McGilp J F and Margaritondo G 1995 *Surf. Sci.* **325** 45
[3] Crain J N, Altmann K N, Bromberger C, Erwin S C, Kirakosian A, McChesney J L, Lin J-L and Himpsel F J 2003 *Phys. Rev. Lett.* **90** 176805
[4] Collazo-Davila C, Grozca D and Marks L D 1998 *Phys. Rev. Lett.* **80** 1678
[5] Lottermoser L, Landemark E, Smilgies D M, Nielsen M, Feidenhans'l R, Falkenberg G, Johnson L, Gierer M, Seitsonen A P and Kleine H 1998 *Phys. Rev. Lett.* **80** 3980
[6] Erwin S C and Weitering H H 1998 *Phys. Rev. Lett.* **81** 2296
[7] Sakamoto K, Ashima H, Zhang H M and Uhrberg R I G 2001 *Phys. Rev.* B **65** 045305

[8] Gurnett M, Gustafsson J B, Magnusson K O, Widstrand S M and Johansson L S O 2002 *Phys. Rev.* B **66** 161101
[9] Hirayama H, Horie R and Takayanagi K 2001 *Surf. Sci.* **482** 1277
[10] Kuntze J, Mugarza A and Ortega J E 2002 *Appl. Phys. Lett.* **81** 2463
[11] O'Mahony J D, McGilp J F, Leibsle F M, Weightman P and Flipse C F J 1993 *Semicond. Sci. Technol.* **8** 495
[12] Aspnes D E and Studna A A 1985 *Phys. Rev. Lett.* **17** 1956
[13] Weightman P, Martin D S, Cole R J and Farrell T 2005 *Rep. Prog. Phys.* **68** 1251
[14] Fleischer K, Chandola S, Esser N, Richter W and McGilp J F 2001 *Phys. Status Solidi* a **188** 1411
[15] Yasuda T, Aspnes D E, Lee D R, Bjorkman C H and Lukovsky G 1994 *J. Vac. Sci. Technol.* A **12** 1152
[16] Borenzstein Y and Alameh R 1992 *Surf. Sci.* **274** L509
[17] Chandola S, Jacob J, Fleischer K, Vogt P, Richter W and McGilp J F 2005 *Phys. Status Solidi* b **242** 3017
[18] Wang S, Lu W, Schmidt W G and Bernholc J 2003 *Phys. Rev.* B **68** 035329
[19] Bennett H E and Bennett J M 1966 *Optical Properties and Electronic Structure of Metals and Alloys* ed F Abeles (Amsterdam: North-Holland) p 181
[20] Fuster G, Tyler J M, Brener N E, Callaway J and Bagayoko D 1990 *Phys. Rev.* B **42** 7322
[21] Shiang J J, Heath J R, Collier C P and Saykally R J 1998 *J. Phys. Chem.* B **102** 3425
[22] Fleischer K, Chandola S, Esser N and McGilp J F 2005 *Phys. Status Solidi* b **242** 2655
[23] Stroud D 1979 *Phys. Rev.* B **19** 1783
[24] Rao C N R, Kulkarni G U, Govindaraj A, Satishkumar B C and John Thomas P 2000 *Pure Appl. Chem.* **72** 21
[25] Lai X, St Clair T P, Valden M and Goodman D W 1999 *Prog. Surf. Sci.* **59** 25
[26] Park K-H, Shin M, Ha J S, Yun W S and Ko Y-J 1999 *Appl. Phys. Lett.* **75** 139
[27] Kirakosian A, Crain J N, Lin J-L, McChesney J L, Petrovykh D Y, Himpsel F J and Bennewitz R 2003 *Surf. Sci.* **532–535** 928
[28] Ekhardt W 1997 *Z. Phys.* B **103** 305